

Improving the Fidelity of Optical Zeno Gates via Distillation

Patrick M. Leung* and Timothy C. Ralph
Centre for Quantum Computer Technology, Department of Physics,
University of Queensland, Brisbane 4072, Australia
(Dated: October 31, 2018)

We have modelled the Zeno effect Control-Sign gate of Franson et al (PRA 70, 062302, 2004) and shown that high two-photon to one-photon absorption ratios, κ , are needed for high fidelity free standing operation. Hence we instead employ this gate for cluster state fusion, where the requirement for κ is less restrictive. With the help of partially offline one-photon and two-photon distillations, we can achieve a fusion gate with unity fidelity but non-unit probability of success. We conclude that for $\kappa > 2200$, the Zeno fusion gate will out perform the equivalent linear optics gate.

PACS numbers: 03.67.Lx, 42.50.-p

INTRODUCTION

Quantum bits (qubits) based on polarization or spatial degrees of freedom of optical modes have several advantages: they are easily manipulated and measured; they exist in a low noise environment and; they are easily communicated over comparatively long distances. Recently considerable progress has been made on implementing two qubit gates in optics using the measurement induced non-linearities proposed by Knill, Laflamme and Milburn [1]. Non-deterministic experimental demonstrations have been made [2, 3, 4] and theory has found significant ways to reduce the resource overheads [5, 6, 7, 8]. Nevertheless, the number of photons and gate operations required to implement a near deterministic two qubit gate remains high.

A possible solution to this problem is the optical quantum Zeno gate suggested by Franson et al [9], [10]. This gate uses passive two-photon absorption to suppress gate failure events associated with photon bunching at the linear optical elements, using the quantum Zeno effect [11]. In principle a near deterministic, high fidelity control-sign (CZ) gate can be implemented between a pair of photonic qubits in this way. However, the slow convergence of the Zeno effect to the ideal result, with ensuing loss of fidelity, and the effect of single photon loss raises questions about the practicality of this approach.

Here we consider a model of the gate that includes the effects of finite two-photon absorption and non-negligible single photon absorption. We obtain analytic expressions for the fidelity of the gate and its probability of success in several scenarios and show how the inclusion of optical distilling elements [12] can lead to high fidelity operation under non-ideal conditions for tasks such as cluster state construction [6].

The paper is arranged in the following way. We begin in the next section by introducing our model in an idealized and then more realistic setting and obtain results for a free-standing CZ gate. In section 3 we focus on using the gate as a fusion element [8] for the construction of, for example, optical cluster states.

We introduce a distillation protocol that significantly improves the operation of the gate in this scenario. In section 4 we summarize and conclude.

MODEL OF ZENO CZ GATE

Franson et al [9] suggested using a pair of optical fibres weakly evanescently coupled and doped with two-photon absorbing atoms to implement the gate. As the photons in the two fibre modes couple the occurrence of two photon state components is suppressed by the presence of the two-photon absorbers via the Zeno effect. After a length of fibre corresponding to a complete swap of the two modes a π phase difference is produced between the $|11\rangle$ term and the others. If the fibre modes are then swapped back by simply crossing them, a CZ gate is achieved.

We model this system as a succession of n weak beamsplitters followed by 2-photon absorbers as shown in Fig. 1. As $n \rightarrow \infty$ the model tends to the continuous coupling limit envisaged for the physical realization. The gate operates on the single-rail encoding [13] for which $|0\rangle_L = |0\rangle$ and $|1\rangle_L = |1\rangle$ with the kets representing photon Fock states. Fig. 2 shows how the single rail CZ can be converted into a dual rail CZ with logical encoding $|0\rangle_L = |H\rangle = |10\rangle$ and $|1\rangle_L = |V\rangle = |01\rangle$ with $|ij\rangle$ a Fock state with i photons in the horizontal polarization mode and j photons in the vertical.

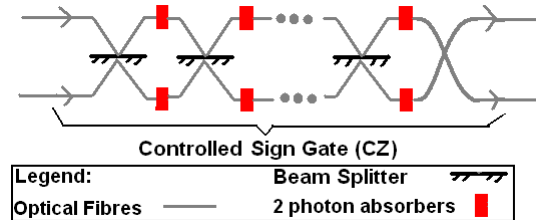


FIG. 1: Construction of our CZ gate.

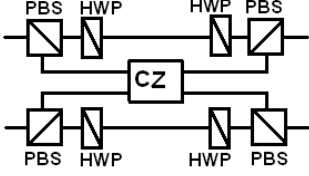


FIG. 2: CZ gate in dual rail implementation.

The general symmetric beam splitter matrix has the form:

$$e^{i\delta} \begin{bmatrix} \cos \theta & \pm i \sin \theta \\ \pm i \sin \theta & \cos \theta \end{bmatrix}$$

According to Figure 1, after the first beam splitter, the four computational photon number states become:

$$\begin{aligned} |00\rangle &\rightarrow |00\rangle \\ |01\rangle &\rightarrow e^{i\delta}(\cos \theta|01\rangle \pm i \sin \theta|10\rangle) \\ |10\rangle &\rightarrow e^{i\delta}(\pm i \sin \theta|01\rangle + \cos \theta|10\rangle) \\ |11\rangle &\rightarrow e^{i2\delta}(\cos 2\theta|11\rangle \pm \frac{i}{\sqrt{2}} \sin 2\theta(|02\rangle + |20\rangle)) \end{aligned} \quad (1)$$

Ideal Two-Photon Absorption

To illustrate the operation of the gate we first assume ideal two-photon absorbers, i.e. they completely block the two-photon state components but do not cause any single photon loss. Propagation through the first pair of ideal two-photon absorbers gives the mixed state

$$\rho^{(1)} = P_s^{(1)}|\phi\rangle^{(1)}\langle\phi|^{(1)} + P_f^{(1)}|vac\rangle\langle vac| \quad (2)$$

where $|\phi\rangle^{(1)}$ is the evolved two-mode input state obtained for the case of no two-photon absorption event and $|vac\rangle$ is the vacuum state obtained in the case a two-photon absorption event occurs. The individual components of $|\phi\rangle^{(1)}$ transform as

$$\begin{aligned} |00\rangle &\rightarrow |00\rangle \\ |01\rangle &\rightarrow e^{i\delta}(\cos \theta|01\rangle \pm i \sin \theta|10\rangle) \\ |10\rangle &\rightarrow e^{i\delta}(\pm i \sin \theta|01\rangle + \cos \theta|10\rangle) \\ |11\rangle &\rightarrow e^{i2\delta} \cos 2\theta|11\rangle \end{aligned} \quad (3)$$

Notice that, because we are embedded in a dual rail circuit, we can distinguish between the $|00\rangle$ state that corresponds to input state $|HH\rangle$ and the $|vac\rangle$ state that results from two-photon absorption of input state $|VV\rangle$.

Equation (3) describes the transformation of each unit, hence repeating the procedure n times gives,

$$\begin{aligned} |00\rangle &\rightarrow |00\rangle \\ |01\rangle &\rightarrow e^{in\delta}(\cos n\theta|01\rangle \pm i \sin n\theta|10\rangle) \\ |10\rangle &\rightarrow e^{in\delta}(\pm i \sin n\theta|01\rangle + \cos n\theta|10\rangle) \\ |11\rangle &\rightarrow e^{i2n\delta}(\cos 2\theta)^n|11\rangle \end{aligned} \quad (4)$$

describing the transformations giving the evolved input state after n units, $|\phi\rangle^{(n)}$. There are three conditions to satisfy for building a CZ gate. The first condition is “ $n\theta = \frac{\pi}{2}$ ”, so that $|01\rangle \rightarrow e^{i(n\delta \pm \frac{\pi}{2})}|10\rangle$ and $|10\rangle \rightarrow e^{i(n\delta \pm \frac{\pi}{2})}|01\rangle$. The second condition is “ $n\delta \pm \frac{\pi}{2} = k\pi$ ” (equivalently, $\delta = \frac{\pi}{2n} + \frac{k\pi}{n}$), where k is any integer, so that $|10\rangle \rightarrow e^{ik\pi}|01\rangle$ and $|01\rangle \rightarrow e^{ik\pi}|10\rangle$ and $|11\rangle \rightarrow -(\cos 2\theta)^n|11\rangle$. Phase shifters are needed to correct the sign of the output state of $|01\rangle$ and $|10\rangle$ for odd k , but here we simply set $k = 0$. The last condition is “ $\cos 2\theta > 0$ ” (i.e. $0 < \theta < \frac{\pi}{4}$), such that a minus sign is induced on $|11\rangle$. This condition is always true because we are using many weak beam splitters (i.e. θ is small). Let $\tau = (\cos 2\theta)^n = (\cos \frac{\pi}{n})^n \geq 0$, then swapping the fibres gives the transformations

$$\begin{aligned} |00\rangle &\rightarrow |00\rangle \\ |01\rangle &\rightarrow |01\rangle \\ |10\rangle &\rightarrow |10\rangle \\ |11\rangle &\rightarrow -\tau|11\rangle \end{aligned} \quad (5)$$

Clearly, the above is a controlled sign operation with a skew (quantified as τ) on the probability amplitude of the $|11\rangle$ state. If there is some way to herald failure, i.e. two-photon absorption events, then the fidelity of the gate will be $F_h = |\langle T|\phi\rangle^{(n)}|^2$, where $|T\rangle$ is the target state, and the probability of success will be $P_s^{(n)}$. On the other hand if two-photon absorption events are unheralded then the fidelity will be $F_{uh} = F_h P_s^{(n)}$. For simplicity we consider the equally weighted superposition input state $\frac{1}{2}(|00\rangle + |01\rangle + |10\rangle + |11\rangle)$. The corresponding $|\phi\rangle^{(n)}$ after the Zeno-CZ gate is $\frac{1}{2}(|00\rangle + |01\rangle + |10\rangle - \tau|11\rangle)$, to be compared with the target state $|T\rangle = \frac{1}{2}(|00\rangle + |01\rangle + |10\rangle - |11\rangle)$. The heralded fidelity and probability of success are then $F_h = \frac{(3+\tau)^2}{4(3+\tau^2)}$ and $P_s = \frac{3+\tau^2}{4}$ respectively. As n becomes very large and hence tends to the continuous limit, τ tends to one, and so both F_h and P_s approach one.

Incomplete Two-Photon Absorption with Single Photon Loss

The previous analysis is clearly unrealistic as it assumes infinitely strong two-photon absorption but negligible single photon absorption. We now include the effect of finite two-photon absorption and non-negligible single photon loss. Let $\gamma_1 = \exp(-\frac{\lambda}{n\kappa})$ and $\gamma_2 = \exp(-\frac{\lambda}{n})$ be the probability of single photon and two-photon transmission respectively for one absorber. Here the parameter $\lambda = \chi L$, where L is the length of the absorber and χ is the corresponding proportionality constant related to the absorption cross section. Furthermore, κ specifies the relative strength of the two transmissions and relates them by $\gamma_2 = \gamma_1^\kappa$. Now each unit of weak beam splitter

and absorbers does the following transformation on the computational states of $|\phi\rangle$

$$\begin{aligned}
|00\rangle &\rightarrow |00\rangle \\
|01\rangle &\rightarrow e^{i\delta}\sqrt{\gamma_1}(\cos\theta|01\rangle \pm i\sin\theta|10\rangle) \\
|10\rangle &\rightarrow e^{i\delta}\sqrt{\gamma_1}(\pm i\sin\theta|01\rangle + \cos\theta|10\rangle) \\
|11\rangle &\rightarrow e^{i2\delta}\gamma_1(\cos 2\theta|11\rangle \pm \frac{i\sqrt{\gamma_2}\sin 2\theta}{\sqrt{2}}(|02\rangle + |20\rangle)) \\
|02\rangle &\rightarrow e^{i2\delta}\gamma_1(\frac{\pm i\sin 2\theta}{\sqrt{2}}|11\rangle + \sqrt{\gamma_2}(\cos^2\theta|02\rangle - \sin^2\theta|20\rangle)) \\
|20\rangle &\rightarrow e^{i2\delta}\gamma_1(\frac{\pm i\sin 2\theta}{\sqrt{2}}|11\rangle - \sqrt{\gamma_2}(\sin^2\theta|02\rangle - \cos^2\theta|20\rangle))
\end{aligned} \tag{6}$$

Repeating the procedure n times with the aforementioned conditions on θ gives the following

$$\begin{aligned}
|00\rangle &\rightarrow |00\rangle \\
|01\rangle &\rightarrow \gamma_1^{n/2}|01\rangle \\
|10\rangle &\rightarrow \gamma_1^{n/2}|10\rangle \\
|11\rangle &\rightarrow -\gamma_1^n\tau|11\rangle + f(|02\rangle, |20\rangle)
\end{aligned} \tag{7}$$

where the new expression for τ is given by:

$$\begin{aligned}
\tau_{n,\lambda} &= \frac{2^{-\frac{3}{2}-n}}{d} \left((g + \frac{d}{\sqrt{2}})^n (\sqrt{2}d - h) \right. \\
&\quad \left. + (g - \frac{d}{\sqrt{2}})^n (\sqrt{2}d + h) \right) \\
d_{n,\lambda} &= \sqrt{(1 + \cos \frac{2\pi}{n})(1 + \gamma_2) + 2\sqrt{\gamma_2}(\cos(\frac{2\pi}{n}) - 3)} \\
g_{n,\lambda} &= (\cos \frac{\pi}{n})(\sqrt{\gamma_2} + 1) \\
h_{n,\lambda} &= 2(\cos \frac{\pi}{n})(\sqrt{\gamma_2} - 1)
\end{aligned} \tag{8}$$

and we have suppressed the explicit form of the $|02\rangle, |20\rangle$ state components as they lie outside the computational basis and so do not explicitly contribute to the fidelity. These expressions can be used to calculate the unheralded fidelity, the heralded fidelity and probability of success. Our numerical evaluations are all carried out in the (near) continuous limit of large n .

Free Standing Gate

For a free-standing gate, as depicted in Fig.2, gate failure events are not heralded, thus the unheralded fidelity is appropriate to consider. The fidelity is a function of λ . As the length of the interaction region is increased (λ increased) the effective strength of the two-photon absorption is increased leading to an improvement in the heralded fidelity, F_h . However, at

the same time, the level of single photon absorption is also increasing with the length, acting to decrease the probability of success, P_s . As the unheralded fidelity is $F_{uh} = F_h P_s$, there is a trade-off between these two effects leading to an optimum value for λ for sufficiently large κ . An example of the dependence is shown in Fig.3. The fidelity is plotted as a function of κ with λ optimized for each point in Fig.4. For large ratios of two-photon absorption to single-photon absorption, κ , we tend to the ideal case of unit fidelity. However, the conditions required are demanding with absorption ratios of a million to one required for $F_{uh} > 0.99$ and 100 million to one for $F_{uh} > 0.999$. Recent estimates suggest κ 's of ten thousand to one may be achievable [14], well short of these numbers. In the following we will consider a different scenario in which the gate can be usefully employed with less stringent conditions on κ .

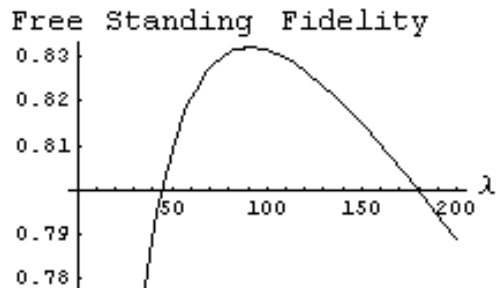


FIG. 3: Unheralded fidelity versus λ for the CZ gate shown in Fig.2. Here $\kappa = 1000$.

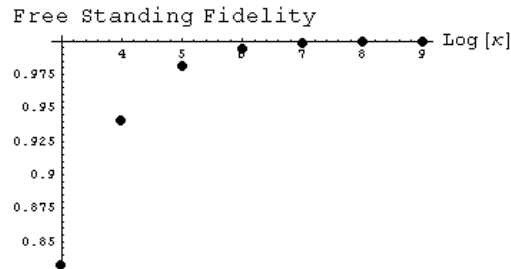


FIG. 4: Unheralded fidelity versus $\text{Log}(\kappa)$ (in base 10) for the CZ gate shown in Fig.2, where we have used the optimal values of λ .

ZENO FUSION GATE

We have seen that the requirements on high fidelity operation for the free-standing gate are quite extreme. We now consider an alternate scenario in which probability of success is traded-off against fidelity by heralding failure events through direct detection. In particular we consider using the Zeno gate to implement the fusion

technique [8]. Fusion can be used to efficiently construct cluster states [15], or re-encode parity states [16]. We will specifically consider cluster state construction here. Essentially, the gate is used to make a Bell measurement on a pair of qubits, as depicted in Fig.9. One of the qubits comes from the cluster we are constructing, whilst the other comes from a resource cluster state, in a known logical state. The Bell measurement has the effect of “fusing” the resource state onto the existing state. By careful choice of the resource state, large 2-dimensional cluster states, suitable for quantum computation, can be constructed [17]. Because the Bell measurement ends with the direct detection of the qubits, the loss of one or both of the photons, or the bunching of two photons in a single qubit mode can immediately be identified in the detection record, and hence failure events will be heralded. Effectively we will postselect the density operator $\rho = P_s |\phi'\rangle\langle\phi'| + \rho_r$, where $|\phi'\rangle$ is the component of the output state which remains in the computational basis and ρ_r are all the components that do not. The measurement record then allows us to herald the first term of the density operator as successful operation, with fidelity $F_h = |\langle T|\phi'\rangle|^2$ and probability of success of P_s , and the second term as failure. We now consider techniques for improving the heralded fidelity of the gate and then evaluate its performance as a fusion gate.

Single Photon Distillation

From equation (7), we can see that $\gamma_1 < 1$ lowers the probability amplitude of the four computational states unevenly as previously discussed by Jacobs et al [10]. By distilling the states with beam splitters and detectors [12] (see Figure 5), where each beam splitter has a transmission coefficient equal to $\gamma_1^{n/2}$, the four computational states of $|\phi'\rangle$ become:

$$\begin{aligned} |00\rangle &\rightarrow \gamma_1^n |00\rangle \\ |01\rangle &\rightarrow \gamma_1^n |01\rangle \\ |10\rangle &\rightarrow \gamma_1^n |10\rangle \\ |11\rangle &\rightarrow -\gamma_1^n \tau |11\rangle \end{aligned} \quad (9)$$

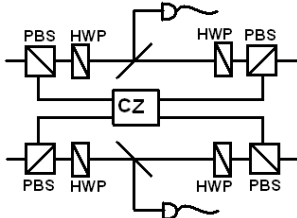


FIG. 5: CZ gate in dual rail implementation with beam splitter distillation to improve average fidelity.

The distillation is successful when the (ideal) detectors measure no photon. The fidelity and probabil-

ity of success of this scheme are $F_h = \frac{(3+\tau)^2}{4(3+\tau^2)}$ and $P_s = \gamma_1^{2n} \left(\frac{3+\tau^2}{4}\right) = e^{-2\lambda/\kappa} \left(\frac{3+\tau^2}{4}\right)$ respectively.

For λ tends to infinity $F_h \rightarrow 1$, however at the same time $P_s \rightarrow 0$. In order to achieve unit fidelity *independent* of λ , we now apply two-photon distillation.

Two-Photon Distillation

As shown previously, after the CZ gate and single photon distillation, the input state $\frac{1}{2}(|00\rangle + |01\rangle + |10\rangle + |11\rangle)$ becomes $\frac{\gamma_1^n}{2}(|00\rangle + |01\rangle + |10\rangle - \tau|11\rangle)$. Now we require two-photon distillation to renormalise the input state by inducing τ on the other three computational states as shown in Figure 6. To do so, we first apply a bit-flip on the control qubit and then apply a τ -gate (see Figure 8) and a single photon distiller on the control qubit with transmission coefficient $\sqrt{\gamma_1}$ and another single photon distiller on the target qubit with transmission coefficient $\sqrt{\gamma_1}\tau$ and then undo the previous bit-flip by applying another bit-flip on the control qubit. The τ -gate does the same operation as the aforementioned CZ gate (excluding the single photon distillation) except that no minus sign is induced on the output of $|11\rangle$. The construction of a τ -gate is described in the next subsection. In summary the two-photon distillation circuit does the following:

$$\begin{aligned} |00\rangle &\rightarrow \gamma_1' \tau |00\rangle \\ |01\rangle &\rightarrow \gamma_1' \tau |01\rangle \\ |10\rangle &\rightarrow \gamma_1' \tau |10\rangle \\ |11\rangle &\rightarrow \gamma_1' |11\rangle \end{aligned} \quad (10)$$

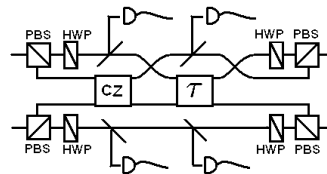


FIG. 6: Two-photon distillation. Schematic of operation sequence, CZ gate, bit-flip, τ -gate with two single photon distillers and then bit-flip.

After the above operations, the input state $\frac{1}{2}(|00\rangle + |01\rangle + |10\rangle + |11\rangle)$ becomes $\frac{\gamma_1^n \gamma_1' \tau}{2}(|00\rangle + |01\rangle + |10\rangle - |11\rangle)$. Now the state can be renormalised to achieve unit fidelity *independent* of λ . The explicit expression for the probability of success is $P_s = \gamma_1^{2n} \gamma_1'^2 \tau^2 = e^{-2\lambda/\kappa} \tau^2 + 2/\kappa$. Figure 7 shows the probability of success of this gate for different values of κ .

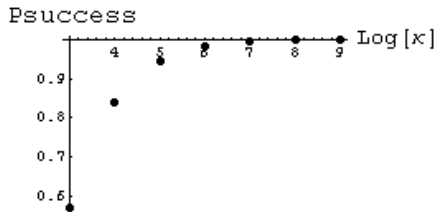


FIG. 7: Probability of success of the CZ gate with two-photon and single photon distillation plotted against $\log \kappa$ (in base 10). Fidelity is always one.

The τ -Gate Circuit

We can construct a τ -gate with two 50-50 beam splitters, a pair of two-photon absorbers, and some phase shifters, as shown in Figure 8. The first beam splitter performs $|01\rangle \rightarrow |10\rangle$, $|10\rangle \rightarrow |01\rangle$ and $|11\rangle \rightarrow \frac{i}{\sqrt{2}}(|02\rangle + |20\rangle)$. The pair of two-photon absorbers then induce $\sqrt{\gamma'_1}$ on both $|01\rangle$ and $|10\rangle$ due to single photon loss, and induce $\gamma'_1\gamma'_2$ on $\frac{i}{\sqrt{2}}(|02\rangle + |20\rangle)$ due to both single photon and two-photon loss. The second beam splitter undoes the operation of the first beam splitter. Then with some phase shifters to correct the relative phase between the terms and having $\gamma'_1\kappa = \gamma'_2 = \tau$, we have a τ -gate that does the following operation:

$$\begin{aligned}
 |00\rangle &\rightarrow |00\rangle \\
 |01\rangle &\rightarrow \sqrt{\gamma'_1}|01\rangle \\
 |10\rangle &\rightarrow \sqrt{\gamma'_1}|10\rangle \\
 |11\rangle &\rightarrow \gamma'_1\tau|11\rangle
 \end{aligned} \tag{11}$$

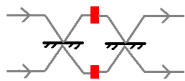


FIG. 8: τ -gate.

Performance of the Zeno Fusion Gate

The fusion approach is important because it is the most efficient method known for performing quantum computation using only linear optics. Linear optics allows a partial Bell measurement to be made with a probability of success of 50% (assuming ideal detectors). In addition the failure mode measures the qubits in the computational basis, which does not affect the state of the remaining qubits in the cluster or parity state. Thus a failure event only sacrifices a single qubit from the cluster being constructed and the probability of destroying N qubits in the process of achieving a

successful fusion is $P_l = 2^{-N}$. In contrast, many of the failure events for the Zeno gate will simply erase the photon giving no knowledge about its state. For simplicity, and to be conservative, we will assume all events lead to complete erasure of the photon state. In order to recover from this situation the adjoining qubit in the cluster must be measured in the logical basis, thus removing the affect of the erasure [18, 19]. This means that every failure event sacrifices two qubits from the cluster being constructed and the probability of destroying N qubits in the process of achieving a successful fusion is $P_z = (1 - P_s)^{N/2}$. Requiring $P_l = P_z$ we estimate that the Zeno gate must have $P_s > 0.75$ to offer an advantage over linear optics.

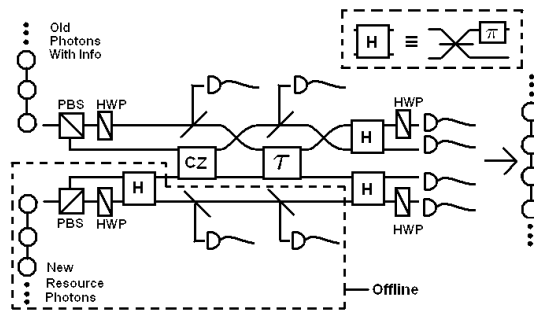


FIG. 9: Zeno Fusion gate with partial offline distillation.

We can make one final improvement to the set-up by relocating the distillation process for the resource qubit to offline (see Fig.5), which boosts the probability of success. The probability of success is then given by $P = \frac{2\gamma_1^{2n}\gamma_1'^2\tau^2}{1+\gamma_1^n\gamma_1'\tau} = \frac{2e^{-2\lambda/\kappa}\tau^{(2+2/\kappa)}}{1+e^{-\lambda/\kappa}\tau^{(1+1/\kappa)}}$. The plot for the probability of success versus κ and optimal λ versus κ are shown in Figure 10 and Figure 11 respectively.

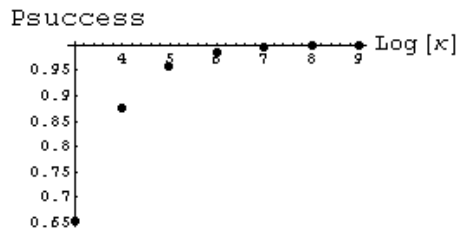


FIG. 10: Probability of success of the Zeno fusion gate with partially offline two-photon and single photon distillation plotted against $\log \kappa$ (in base 10).

The break even point between linear optics and the Zeno gate is when $\kappa = 2200$, such that the probability of success is about 0.75. When $\kappa = 10000$ the probability of success is about 0.87. Thus we conclude that an absorption ratio of ten thousand to one or more would produce a Zeno gate with significant advantage over linear fusion techniques.

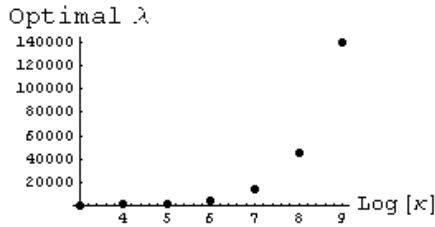


FIG. 11: Optimal λ for the probability of success of the Zeno fusion gate with partially offline two-photon and single photon distillation plotted against $\log \kappa$ (in base 10).

Conclusion

In this paper, we have modelled Franson et al's CZ gate with a succession of n weak beam-splitters followed by two-photon absorbers, in the (near) continuous limit of large n . We analysed this CZ gate for both the ideal two-photon absorption case and the incomplete two-photon absorption with single photon loss case, giving analytical and numerical results for the fidelity and probability of success. The result shows that for a free-standing gate we need an absorption ratio κ of a million to one to achieve $F > 0.99$ and 100 million to one to achieve $F > 0.999$, where recent estimate only suggests that $\kappa \approx 10000$ may be achievable. We therefore employ this gate for qubit fusion, where the requirement for κ is less restrictive. With the help of partially offline one-photon and two-photon distillations, we can achieve a CZ gate with unity fidelity and with probability of success is about 0.87 for $\kappa = 10000$. We conclude that when employed as a fusion gate, the Zeno gate could offer significant advantages over linear techniques for reasonable parameters.

Acknowledgement

We thank W.J.Munro, A.Gilchrist and C.Myers for useful discussions. This work was supported by the

Australian Research Council and the DTO-funded U.S. Army Research Office Contract No. W911NF-05-0397.

* Electronic address: pmleung@physics.uq.edu.au

- [1] E. Knill, R. Laflamme, and G.J. Milburn, *Nature* **409**, 46-52 (2001).
- [2] J.L.O'Brien, G.J.Pryde, A.G.White, T.C.Ralph, D.Branning, *Nature* **426**, 264(2003).
- [3] T.B. Pittman, M.J. Fitch, B.C. Jacobs, and J.D. Franson, *Phys. Rev. A* **68**, 032316 (2003).
- [4] S.Gasparoni, J.-W.Pan, P.Walther, T.Rudolph, and A.Zeilinger *Phys. Rev. Lett.* **93**, 020504 (2004).
- [5] N.Yoran and B.Reznik, *Phys. Rev. Lett.* **91**, 037903 (2003).
- [6] M.A. Nielsen, *Phys. Rev. Lett.* **93**, 040503 (2004).
- [7] A.J.F.Hayes, A.Gilchrist, C.R.Myers and T.C.Ralph, *J.Opt.B* **6**, 533 (2004).
- [8] D.E.Browne and T.Rudolph, *Phys. Rev. Lett.* **95**, 010501 (2005).
- [9] J.D. Franson, B.C. Jacobs, and T.B. Pittman, *PRA* **70**, 062302 (2004)
- [10] B.C. Jacobs, T.B. Pittman, and J.D. Franson, *PRA* **74**, 010303(R) (2006)
- [11] W. Kaiser and C. Garrett, *PRL* **7** 229 (1961)
- [12] R.T. Thew and W.J. Munro, *PRA* **63**, 030302(R) (2001)
- [13] A.P. Lund, T.C. Ralph, *PRA*, **66**, 032307 (2002).
- [14] J.D. Franson and S.M. Hendrickson *quant-ph* 0603044 (2006)
- [15] R. Raussendorf and H.J. Briegel, *PRL* **86** 5188 (2001)
- [16] T.C. Ralph, A.J.F. Hayes and A. Gilchrist, *PRL* **95** 100501 (2005)
- [17] C.M. Dawson, H.L. Haselgrove, and M.A. Nielsen, *PRL* **96**, 020501 (2006)
- [18] L.M. Duan and R. Raussendorf, *PRL* **95**, 080503 (2005)
- [19] Y.L. Lim, S.D. Barrett, A. Beige, P. Kok, L.C. Kwek, *PRA* **73**, 012304 (2006)